

Comparison of Practical Feedback Algorithms for Multiuser MIMO

Maryam Modir Shanechi, *Member, IEEE*, Ron Porat, *Member, IEEE*, and Uri Erez, *Member, IEEE*

Abstract—We consider the problem of obtaining channel state information (CSI) via a fast feedback link for transmission on the downlink of a multiuser MIMO system. We examine the relative merits of channel feedback schemes based on Shannon's source-channel separation principle (digital schemes) and non-separation based schemes and show that the latter are preferable in this application when small to moderate bandwidth expansion ratios are used as in many current cellular systems. For comparison, we first compute upper-bounds on the performance of the system as a function of SNR. For the non-separation based schemes, we first consider a simple analog transmission and then develop a hybrid digital-analog transmission scheme which quantizes the CSI using a few bits and sends these bits and also the quantization error using analog transmission. We show that the hybrid scheme achieves a higher throughput compared to both analog and digital transmissions and has a much lower computational complexity compared to a digital scheme.

Index Terms—MIMO systems, channel state information (CSI) feedback, joint source-channel coding, multiuser MIMO, analog feedback.

I. INTRODUCTION

IN closed loop multiple-input multiple-output (MIMO) cellular systems, the base station must obtain knowledge of the downlink channel state information (CSI). For single-user MIMO applications, this information is used to direct the transmitted power towards the mobile station and provides an SNR gain which results in significant throughput gains. For multiuser MIMO applications, accurate CSI at the transmitter (CSIT) is of even greater importance [1] since having inaccurate CSIT results in residual interference, incurs a significant loss in throughput, and results in a loss in the multiplexing gain [2], [3]. Obtaining high quality CSIT at the base station is a difficult problem especially in frequency-division duplex (FDD) systems, where channel reciprocity cannot be used and the CSI must be fed back to the base station on a fast feedback link. Hence, designing good channel feedback coding algorithms are of significant interest in such systems.

The channel state information, e.g., the channel matrix, is an analog source in nature. The goal of the feedback algorithm

is to encode this information at the mobile station to enable its reconstruction with minimum distortion at the base station. Thus, the feedback coding problem is a joint source-channel coding problem. In addition, the requirements of low delay dictate the use of short block lengths.

There are two main approaches one could take in designing the CSI feedback link. One that has traditionally received most attention (e.g. [4]–[9]) is based on Shannon's source-channel separation theorem that proves the asymptotic optimality of separate source and channel coding under certain conditions (discussed, e.g., in [10]). In such schemes, which we refer to as "digital schemes", the source (CSI) is first quantized and then the quantized CSI is (possibly) encoded using a channel code to recover the quantized source with low error probability at the receiver. The main drawback of a digital scheme, however, is the threshold effect which means that the system achieves the desired performance only at the designed SNR. At lower SNR, system performance is severely sacrificed and at higher SNR, it does not improve. Hence this approach is suboptimal in a scenario where the exact SNR is known only to lie in some range. Another shortcoming of this approach even for a single (and known) SNR is that long source and channel codes are needed to achieve the optimal performance [10] which is not possible over a fast feedback link.

The other approach one could take to solve this problem is a joint source-channel approach that does not follow the separation principle. The simplest example of such a scheme is analog transmission (as considered in, e.g., [11]–[14]) that allows for a graceful degradation of performance at low SNR and does not saturate at high SNR. However, while it is optimal (when the criterion is that of mean-square error (MSE)) for transmitting a Gaussian source over a Gaussian channel of equal bandwidth, analog transmission is suboptimal when the bandwidths are different [15], [16]. Nonetheless, more advanced joint source-channel coding schemes have been devised that make better use of the available bandwidth than purely analog transmission and at the same time are more robust than separate source and channel coding (over a channel with unknown SNR) and offer better performance for a given delay, e.g., [17]–[20]. It is interesting to note that joint source-channel coding techniques have recently gained attention in the context of wireless MIMO communication [21]–[25]. For example channel-optimized vector quantizers have been used in [21], [22] to combine beamforming with space-time coding for a single-user MIMO system.

Here, we examine the relative merits of separation based and non-separation based approaches in the context of MIMO channel feedback, and observe that the latter are preferable in

Paper approved by N. Jindal, the Editor for MIMO Techniques of the IEEE Communications Society. Manuscript received March 9, 2009; revised November 22, 2009.

This work was presented in part at the IEEE Vehicular Technology Conference, Barcelona, Spain, April, 2009.

M. M. Shanechi is with the Department of Electrical Engineering and Computer Science, Massachusetts Institute of Technology, Cambridge, MA, 02139 USA (e-mail: shanechi@mit.edu).

R. Porat is currently a Principal DSP Engineer at Broadcom Corporation, San Diego, CA, USA (e-mail: rporat@broadcom.com).

U. Erez is with the Department of Electrical Engineering, Tel Aviv University, Ramat Aviv, Israel (e-mail: uri@eng.tau.ac.il).

Digital Object Identifier 10.1109/TCOMM.2010.08.090142

MIMO systems where small to moderate bandwidth expansion ratios are used for feedback transmission on the uplink, as is the case in many current cellular systems such as WiMAX [26]. This constraint in turn stems from the need for efficient resource allocation to the multiple users accessing the uplink channel simultaneously and is also considered in [11], [13], [14].

We note that the purely analog feedback approach and its merits have been considered previously in [11], [14] for a single-user system and in [12], [13] for a multiuser system. However, in [12], [13] no direct comparison is made with a digital feedback approach while in [11], [14], for the single-user system considered (in contrast to multiuser), the comparison is made based on the performance of scalar quantizers or specific vector quantizers. In contrast, in the present work the comparison to a digital feedback scheme (in a multiuser MIMO system) is done by computing upper-bounds on the performance attainable by a digital approach rather than taking any specific quantization scheme as a benchmark. We obtain these upper-bounds by finding the performance of random vector quantizers (random VQ) which has been shown to be very close to that of optimal vector quantizers [8]. Hence the conclusions drawn are more general than in previous works and thus strengthen the case for using non-separation based schemes in setups with small to moderate bandwidth expansion ratios. We also show the threshold effect of the digital approach in our upper-bounds as the uplink channels go into outage. Moreover we compute outage-aware upper-bounds on the performance of the best *variable*-size quantizer, i.e., allowing for quantizers with different sizes to be used at different uplink SNRs.

Another useful upper-bound computed is the random VQ based upper-bound on the sum-rate performance of the system as a function of SNR which shows the best performance possible by a feedback scheme without any constraint such as delay. This upper-bound serves as an important benchmark for any feedback scheme.

Finally we develop a hybrid digital-analog source-channel code for the feedback link and show that it performs close to the system upper-bound and better than pure analog transmission.

Using the above bounds as well as analysis and simulation of non-separation based schemes, we demonstrate that they work well in multiuser MIMO systems without exact knowledge of the SNR. This is in contrast to a digital approach where accurate knowledge of SNR (and selection of a quantizer codebook based on that) is essential in achieving a good performance as shown in [8], [9] and also verified by our computed upper-bounds. In particular, the hybrid scheme developed, performs close to the system upper-bound for a wide SNR range. We also observe that the non-separation based schemes incur a much smaller computational complexity as compared to a purely digital approach.

The subsequent sections of this work are organized as follows. Section II describes the system model and multiuser transmission scheme. Section III describes the method used to find an upper-bound on the sum-rate of the system as a function of SNR. Section IV discusses the already known results on the separation-based schemes [8], [9], describes

a transmission strategy for the system to deal with users in outage, and offers a method to find the corresponding outage-aware upper-bounds on the performance of the digital scheme. Section V introduces the hybrid digital-analog feedback algorithm for multiuser MIMO and compares that with analog transmission. Section VI discusses the simulation results and Section VII contains the concluding remarks.

II. CHANNEL MODEL AND TRANSMISSION SCHEME

We consider a multiuser MIMO system with K users each with N_r antennas and a base station (transmitter) with N_t antennas. The downlink channel model of interest takes the form

$$\mathbf{y}_k = \mathbf{H}_k \mathbf{x} + \mathbf{w}_k, \quad k = 1, \dots, K \quad (1)$$

where channel input \mathbf{x} and channel output at user k , \mathbf{y}_k , are N_t - and N_r -dimensional vectors, respectively, and where the associated noise vectors \mathbf{w}_k are $\mathcal{CN}(0, N_0 \mathbf{I}_{N_r \times N_r})$ and independent. Here, \mathbf{H}_k is the channel matrix from the base station to the k th user whose elements we assume are $\mathcal{CN}(0, 1)$ and independent, i.e., Rayleigh faded. We further assume that the channel evolves according to a block-fading model with independent fades. The channel input is constrained to an average power P , i.e., $E[|\mathbf{x}|^2] = P$ and hence for downlink, $\text{SNR} = P/N_0$. We assume that users have equal power allocation on the downlink and perfect CSI at their receivers (CSIR). In this work we set the number of users equal to the number of transmit antennas which is the regime of interest for most next generation wireless systems [9].

For concreteness, we study the performance of the feedback schemes for a specific (zero-forcing based) transmission approach (similar to the one in [27]), but none of the schemes is specifically tailored to this approach. Our transmission scheme is based on sending a single data stream to each user using the regularized zero-forcing (ZF) beamforming [28], that performs better than ZF beamforming [28], as follows. Our scheme is hence similar to that in [27]. Specifically, assuming K active users in the system and denoting the strongest right singular vector of the k th user by $\mathbf{v}^{(k)}$, the regularized ZF beamformer for user k , which we denote by \mathbf{f}_k , is given by the normalized k th column of the matrix

$$\mathbf{\Omega} = \mathbf{\Gamma}^\dagger \left(\mathbf{\Gamma} \mathbf{\Gamma}^\dagger + \frac{K}{\text{SNR}} \mathbf{I} \right)^{-1}, \quad (2)$$

where $\mathbf{\Gamma} = [\mathbf{v}^{(1)}, \dots, \mathbf{v}^{(K)}]^\dagger$. Hence, $\mathbf{f}_k = \boldsymbol{\omega}_k / \|\boldsymbol{\omega}_k\|$, where $\boldsymbol{\omega}_k$ is the k th column of $\mathbf{\Omega}$. Hence the channel input is given by,

$$\mathbf{x} = \sum_{k=1}^K \sqrt{\frac{P}{K}} \mathbf{f}_k s_k = \sqrt{\frac{P}{K}} \mathbf{F} \mathbf{s} \quad (3)$$

where s_k is the intended symbol for the k th user with $E[s_k s_k^\dagger] = 1$, that is, a single stream is sent to each user and equal power is allocated to all streams, $\mathbf{F} = [\mathbf{f}_1 \dots \mathbf{f}_K]$, and $\mathbf{s} = [s_1 \dots s_K]^t$. ZF beamforming, even though suboptimal, offers a good balance between performance and complexity, and is reasonably close to capacity (achieved by dirty paper coding, see e.g. [29]–[31]) when combined with user selection under the assumption of perfect CSIT [9], [32]. This and the

fact that implementing DPC in practice is more complicated, have led to the widespread use of ZF and regularized ZF beamforming for multiuser MIMO transmission [8], [9], [27].

In the case of channel feedback, $\mathbf{\Gamma}$ in (2) is replaced by the estimated matrix from this feedback, $\hat{\mathbf{\Gamma}} = [\hat{\mathbf{v}}^{(1)}, \dots, \hat{\mathbf{v}}^{(k)}]^\dagger$. We assume equal power allocation is used at the base station for all active users and hence each user only feeds back its strongest right eigenvector.

At the receiver, each user exploits a minimum mean-square error (MMSE) receiver to estimate its data as done in [27], which further mitigates the residual interference from the other users. To concentrate on the effect of feedback schemes, we assume that the receivers have perfect CSIR of the interference terms which could be obtained using a dedicated pilot training period in the downlink. At the k th user, the MMSE receiver is thus given by

$$\mathbf{g}_k = \left(\mathbf{I} + \sum_{i \neq k} \frac{P}{KN_0} \mathbf{H}_k \mathbf{f}_i \mathbf{f}_i^\dagger \mathbf{H}_k^\dagger \right)^{-1} \mathbf{H}_k \mathbf{f}_k$$

which results in the k th user SINR of

$$\text{SINR}_k = \frac{P}{KN_0} \mathbf{f}_k^\dagger \mathbf{H}_k^\dagger \left(\mathbf{I} + \sum_{i \neq k} \frac{P}{KN_0} \mathbf{H}_k \mathbf{f}_i \mathbf{f}_i^\dagger \mathbf{H}_k^\dagger \right)^{-1} \mathbf{H}_k \mathbf{f}_k.$$

Finally, taking the symbols s_1, \dots, s_K to be i.i.d. complex Gaussian, the ergodic system throughput is given by

$$R = E_{\mathbf{H}} \left[\sum_{k=1}^K \log_2(1 + \text{SINR}_k) \right].$$

We assume that the base station has side information of the SINR for the different users — which it can receive in the form of the channel quality indicator (CQI) in practice — and hence can allocate the appropriate rate to each user. Also, similar to other works, e.g. [8], we assume that the feedback for a given block is received instantaneously. This is a reasonable assumption if the feedback time, T_f , is much smaller than the coherence time of the channel, T_c , as is the case in many practical scenarios, especially with low mobility [26], [33].

We simulate the transmission scheme both with and without user selection where the user selection is assumed to be done with perfect knowledge (genie-aided) of the downlink channels and an exhaustive search. Thus, it gives an upper bound on the gain of user selection algorithms.

We compare the different feedback algorithms in the above multiuser setup and in terms of the overall system throughput. Each user transmits its N_t dimensional CSI over $\beta_{fb} N_t$ uses of the uplink channel, where β_{fb} is the bandwidth expansion factor. Note that since the feedback overhead, i.e. $\beta_{fb} N_t$, is the same for all feedback algorithms compared, we don't consider it in throughput calculation.

In this work we assume that the users transmit with one fixed antenna in the uplink (as is the case in most wireless devices) and hence the uplink channel is a $N_t \times 1$ single-input multi-output (SIMO) channel. We consider both an unfaded SIMO Gaussian uplink and a more realistic Rayleigh slow-fading SIMO Gaussian uplink generated according to the power delay profile of the ITU Pedestrian B channel [33]

and simulated using a modified Jakes model for Rayleigh fading as in [34]. We assume an uplink SNR of SNR_{UL} with an SNR offset between downlink and uplink of ΔSNR dB = SNR dB - SNR_{UL} dB. Note that the unfaded SIMO Gaussian uplink channel is equivalent to an AWGN uplink channel with $N_t \text{SNR}_{UL}$ and hence we will equivalently refer to it as an AWGN uplink channel. The SNR offset between the uplink and downlink is due to the difference in transmit power between the base station and the mobile station and also their transmission bandwidth. For example for a typical macro-cell cellular deployment over 10 MHz, the base station power is about 23 dB higher than the mobile station [35]. However, while the base station transmits over the entire bandwidth, the mobile station usually uses only a fraction of it and hence can increase its SNR. For example using 200 kHz (1/50 of entire bandwidth) for uplink transmission results in 6 dB offset between the uplink and downlink SNR.

We now define some basic notation. Unless noted otherwise, all logarithms are base 2 and all symbols denote complex quantities. We use \cdot^\dagger for the conjugate transpose operator and $\|\cdot\|_F$ for the Frobenius norm of a matrix. Vectors and matrices are denoted using bold face lower and upper case characters, random variables are denoted using sans-serif fonts, while sample values use regular (serif) fonts

III. RANDOM VQ UPPER-BOUNDS

In comparing the performance of different feedback algorithms, it is useful to find an upper-bound on the performance of any feedback scheme assuming a hypothetical capacity and rate-distortion achieving feedback link. This means that we assume the feedback channel can support a rate equal to the uplink capacity with zero probability of error and that these bits are used to quantize the source using an optimal vector quantizer which in turn achieves the minimum distortion for that source at the corresponding rate. Since optimal vector quantizers are unknown for this problem, we follow [8] and consider a B bit random VQ in which the 2^B quantizer vectors are chosen from the isotropic distribution on the N_t dimensional unit sphere and has been shown to perform very close to the optimal vector quantizer [8]. Hence to find the upper-bound we need to find the performance of a random VQ with $B = \sum_{i=1}^{\beta_{fb} N_t} C_{UL}^{(k)}(i)$ for the k th user, where $C_{UL}^{(k)}(i) = \log(1 + \text{SNR}_{UL} \|\mathbf{h}_{UL}^{(k)}(i)\|^2)$ is the k th user instantaneous uplink capacity on the i th channel use and $\mathbf{h}_{UL}^{(k)}(i)$ is the instantaneous SIMO uplink channel of the k th user on the i th channel use. Note that here we assume error free transmission of the B bits and hence the only error is the quantization error. To find the performance, we hence exploit the distribution of this error as follows.

A. Simulating a random VQ of Arbitrary Dimension

Here we elaborate on a method of simulating a random VQ of arbitrary size or dimension described in [36]. To find the performance of a random VQ with B bits, we exploit the distribution of the quantization error to run Monte Carlo simulations by injecting noise of the same distribution on the feedback vectors $\mathbf{v}^{(k)}$ s. Consider a B bit vector quantizer

(codebook), $\mathcal{Q} = \{\mathbf{q}_1, \dots, \mathbf{q}_{2^B}\}$ with maximum correlation mapping, i.e.,

$$\hat{\mathbf{v}}^{(k)} = \arg \max_i \|\mathbf{q}_i^\dagger \mathbf{v}^{(k)}\| \quad (4)$$

Assuming that the vector to be quantized is isotropically distributed on the N_t dimensional unit sphere (which is the case here for $\mathbf{v}^{(k)}$ s since the downlink channel is i.i.d. Rayleigh faded [4]), the distribution of the angle between the quantizer and the true vector is derived in [37]. Denoting this angle by $\theta = \angle(\mathbf{v}^{(k)}, \hat{\mathbf{v}}^{(k)})$, $m = \sin^2(\theta)$ has a beta distribution with parameters $N_t - 1, 1$, i.e., $\Pr(m \leq m) = 1 - (1 - m)^{N_t - 1}$.

Now assume that \mathbf{u} is a unit norm vector in the orthogonal subspace to $\mathbf{v}^{(k)}$ and let

$$\tilde{\mathbf{v}}^{(k)} = (\mathbf{v}^{(k)} + a\mathbf{u})/\sqrt{1 + a^2}, \quad (5)$$

where a is a scalar. Then by the Pythagorean theorem,

$$\sin^2 \angle(\mathbf{v}^{(k)}, \tilde{\mathbf{v}}^{(k)}) = \frac{a^2}{1 + a^2}$$

Denoting $s = \sin^2(\angle(\mathbf{v}^{(k)}, \tilde{\mathbf{v}}^{(k)}))$ then $a^2 = s/(1 - s)$. Hence to sample the vectors with the desired distribution on their angle to the true vector, we sample s from the distribution of m and form $\tilde{\mathbf{v}}^{(k)}$ with the corresponding a according to (5). We also have to sample \mathbf{u} uniformly from all orthogonal unit norm vectors to $\mathbf{v}^{(k)}$. To do so we first find an orthonormal basis for the orthogonal subspace, $\mathbf{u}_1, \dots, \mathbf{u}_{N_t - 1}$, and then form their linear combination as follows to get \mathbf{u} :

$$\mathbf{u} = \sum_{i=1}^{N_t - 1} c_i \mathbf{u}_i$$

where $\mathbf{c} = [c_1, \dots, c_{N_t - 1}]$ is a unit norm vector generated by normalizing an i.i.d. Gaussian vector $\mathbf{b} \sim \mathcal{CN}(0, \mathbf{I})$, i.e., $\mathbf{c} = \mathbf{b}/\|\mathbf{b}\|$. Hence \mathbf{u} is uniformly sampled from the unit norm subspace of the orthogonal space since the distribution $\mathcal{CN}(0, \mathbf{I})$ is spherically symmetric. Having samples from both a and \mathbf{u} , we can construct the sample quantized vector, $\hat{\mathbf{v}}^{(k)} = (\mathbf{v}^{(k)} + a\mathbf{u})/\sqrt{1 + a^2}$.

In Section VI we use the above method to find the upper bound on our system and use it to compare the different feedback algorithms.

IV. SEPARATION BASED APPROACHES

Separation based or digital approaches for channel feedback have received the greatest traction so far in the literature, e.g., [4]–[9]. It was shown in [8] that using a digital approach and any fixed number of feedback bits per user and without user selection, the overall system throughput is bounded which results in substantial throughput loss. Fig. 3(a) shows the perfect CSIT and the 4 bit digital regularized ZF throughputs for a 4 antenna transmitter and 4 single antenna users with AWGN uplink channels and no selection (details in Section VI). It can easily be seen that system throughput saturates with increasing SNR. This saturation is the result of the system becoming interference limited [8], [9].

It was shown in [8], [9] that to achieve the full multiplexing gain with a digital approach, the number of feedback bits per user should be increased at least at a rate of $(N_t -$

$1) \log_2(\text{SNR})$. It is important to note however, that in terms of practical implementation, this scheme has the following difficulties. First, the quantization codebook has to be decided based on SNR. In many applications this SNR is known only to lie in some range and the mobile station does not have an accurate estimate of it. Since the performance of the system strongly depends on the correct choice of the number of feedback bits, this incurs a significant loss in practical systems and leads to a conservative design since one has to ensure very small probability of error.

Moreover, the number of bits required for this digital scheme is very large for medium and high SNR. For example, for a 4 antenna base station and 1 antenna users at an SNR of 20dB, at least 20 quantization bits are needed per user [9]. This requires the design of multiple (for different SNRs) good quantization codebooks of very large cardinality which is a difficult problem. Having a large codebook also incurs a large computational complexity on the users for codeword selection and thus codebooks with large cardinality would need to be highly structured. These limitations of separation-based approaches in the context of MIMO channel feedback, motivate the study and design of feedback coding algorithms which do not adhere to the separation principle.

In order to show these shortcomings of the digital approach and compare it to non-separation based algorithms, we need to show the performance of the system using different B bit codebooks across the SNR range of interest. To do this we can simulate any codebook of interest to get the multiuser performance. However, it is difficult to design codebooks of arbitrary size and also computationally costly to run such simulations when the cardinality of these codebooks is large. Hence instead of showing the actual performance of an arbitrary B bit vector quantizer, we show random VQ upper-bounds on it as a function of SNR by assuming error-free transmission of bits. To find these upper-bounds we again exploit the method in Section III-A as we now develop.

A. Error-free Digital Upper-bounds

We can find upper-bounds on the performance of the digital approach assuming error-free transmission of the feedback bits by exploiting the distribution of the quantization error and running Monte Carlo simulations using the procedure in Section III-A, but this time keeping B constant and equal to the number of quantization bits. Again since we assume error free transmission of the B bits, the only error introduced is the quantization error. Hence at low SNR, these upper-bounds are loose since the uplink channel is in outage and the error-free assumption does not hold.

B. Outage-aware Digital Upper-bounds

In order to find tighter upper-bounds at the low SNR regime for the digital approach, we need to devise a strategy to deal with the users in feedback transmission outage in the multiuser MIMO system. In order not to penalize the digital approach heavily when some users are in outage, we assume that the base station can detect these users and during the corresponding slots communicate only to users not in outage. This means that the base station does not waste power to communicate to

the users whose channel feedback has been received in error. This strategy has a strictly better performance than the one used in [9] where the mobile stations detect whether their feedback bits were received in error and then just discard those slots. We again assume error free transmission of the feedback bits for all users not in outage even though short block lengths must be used because of the delay constraints.

To derive this upper-bound, we first calculate the instantaneous uplink capacity for each user and compare it to the number of quantizer bits, B . If $\sum_{i=1}^{\beta_{fb} N_t} C_{UL}^{(k)}(i) < B$, then the k th user is in outage and the base station does not communicate to it during that time slot. After detecting all users in outage, the base station uses the same multiuser MIMO transmission scheme with or without user selection but this time only for users not in uplink outage. As we will see in Section VI, doing so clearly shows the threshold effect of the digital approach. Note that this is still an upper-bound on performance since we assume error-free transmission of the feedback bits whenever a user is not in outage, even though short block lengths must be used.

V. NON-SEPARATION BASED APPROACHES

Here we look at two non-separation based schemes for channel feedback. We first look at an analog transmission scheme and then develop a special hybrid digital-analog feedback algorithm motivated by the source-channel codes in [17]. We will show that both schemes are preferable to a digital scheme in a practical setting and moreover the hybrid algorithm has an advantage over a pure analog approach and could be used to close the gap further with respect to the perfect CSIT case.

A. Analog Feedback Algorithm

In analog transmission, the elements of the CSI are sent over the channel using simple unquantized QAM. For the bandwidth expansion case, i.e., $\beta_{fb} > 1$, the same analog signal is repeated over the channel. At the receiver an MMSE estimator obtains the best estimate of the CSI symbols.

B. Hybrid Feedback Algorithm

Here, we develop the hybrid feedback algorithm. This algorithm is based on first quantizing the CSI using a few bits, sending those using a short (e.g., algebraic) code and then sending the quantization error using analog transmission. Here we explain the algorithm based on feeding back the right singular vectors of each user channel, $\mathbf{V}_k = [\mathbf{v}_1^{(k)} \cdots \mathbf{v}_r^{(k)}]$, where r is the transmission rank. Note that this algorithm is applicable to any other channel feedback quantity conditioned on the existence of good quantizer codebooks for it. The hybrid scheme is shown in Fig. 1 and is an extension of [17], [38] where now the source code is the codebook quantizer for the complex channel matrix and additionally an alignment block is introduced. The hybrid scheme proceeds as follows:

- (1) Decide on the transmission rank, r_{opt} , based on the criterion of interest, e.g., based on the multiuser transmission algorithm (rank 1 in our multiuser transmission scheme).
- (2) For each user, quantize $\mathbf{V}_k = [\mathbf{v}_1^{(k)} \cdots \mathbf{v}_{r_{\text{opt}}}^{(k)}]$ using a B bit codebook, $\mathcal{Q} = \{\mathbf{Q}_1, \cdots, \mathbf{Q}_{2^B}\}$, with the mapping

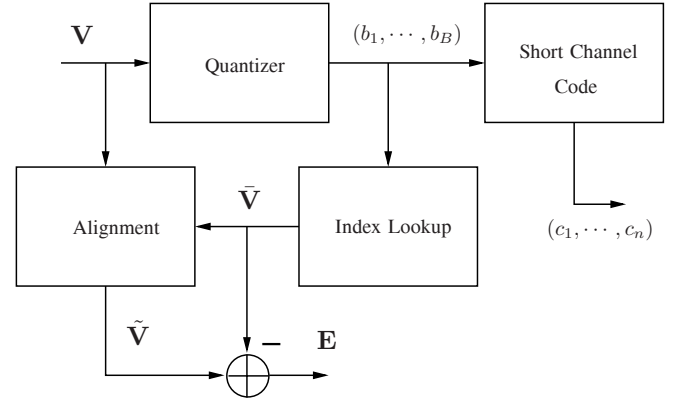


Fig. 1. Hybrid Feedback Algorithm.

criterion of interest such as the maximum correlation criterion [4], i.e.,

$$\bar{\mathbf{V}}_k = \arg \max_i \|\mathbf{Q}_i^\dagger \mathbf{V}_k\|_F. \quad (6)$$

Denote the resulting quantization bits by $(b_1^{(k)}, \cdots, b_B^{(k)})$.

- (3) Align \mathbf{V}_k to $\bar{\mathbf{V}}_k$ by performing a unitary transformation from right on \mathbf{V}_k . To understand the need for this step, first note that the transmission scheme (and capacity of the channel) is invariant to a unitary transformation from right on \mathbf{V}_k for any user (for example for the one dimensional rank 1 transmission this is just an equal phase rotation on every element of $\mathbf{v}^{(k)}$ which does not affect its direction). Also, the quantizer matrix selected for \mathbf{V}_k and any $\mathbf{V}_k \Phi$ with unitary Φ will be the same as apparent from (6). However, in the hybrid scheme, we are also sending back the quantization error in analog form. Applying a unitary transformation from right on \mathbf{V}_k , this quantization error is given by $\bar{\mathbf{V}}_k - \mathbf{V}_k \Phi$ with unitary Φ . Looking at the norm of this error, i.e., $\|\bar{\mathbf{V}}_k - \mathbf{V}_k \Phi\|_F$, it greatly depends on the unitary transformation Φ . Since we want the quantization error variance to be as small as possible to minimize its MSE after reconstruction, we define the distance between \mathbf{V}_k and $\bar{\mathbf{V}}_k$ as

$$d(\mathbf{V}_k, \bar{\mathbf{V}}_k) = \min_{\Phi \in \mathcal{U}} \|\bar{\mathbf{V}}_k - \mathbf{V}_k \Phi\|_F,$$

where \mathcal{U} is the set of all unitary matrices. Our goal is then to find the $\Phi_{\text{opt}}^{(k)}$ that minimizes this distance, i.e., for the k th user

$$\Phi_{\text{opt}}^{(k)} = \arg \min_{\Phi \in \mathcal{U}} \|\bar{\mathbf{V}}_k - \mathbf{V}_k \Phi\|_F^2. \quad (7)$$

We prove in the Appendix that this transformation is given by $\Phi_{\text{opt}}^{(k)} = \mathbf{V}_{\text{corr}} \mathbf{U}_{\text{corr}}^\dagger$ where \mathbf{V}_{corr} and \mathbf{U}_{corr} are the right and left singular vectors of the correlation matrix $\bar{\mathbf{V}}_k^\dagger \mathbf{V}_k$, respectively, i.e., $\bar{\mathbf{V}}_k^\dagger \mathbf{V}_k = \mathbf{U}_{\text{corr}} \Sigma \mathbf{V}_{\text{corr}}^\dagger$ with Σ the diagonal matrix of singular values. We denote the aligned \mathbf{V}_k by $\tilde{\mathbf{V}}_k = \mathbf{V}_k \Phi_{\text{opt}}^{(k)}$.

For example for our rank 1 transmission, $\Phi_{\text{opt}}^{(k)}$ is just a phase rotation on every element by $-\angle(\bar{\mathbf{v}}^{(k)\dagger} \mathbf{v}^{(k)})$.

- (4) Construct the correction or error signal, $\mathbf{E}_k = \bar{\mathbf{V}}_k - \tilde{\mathbf{V}}_k$.
- (5) Possibly use a short channel code (e.g. a (n, B, d) algebraic code such as a Reed Muller code) to encode

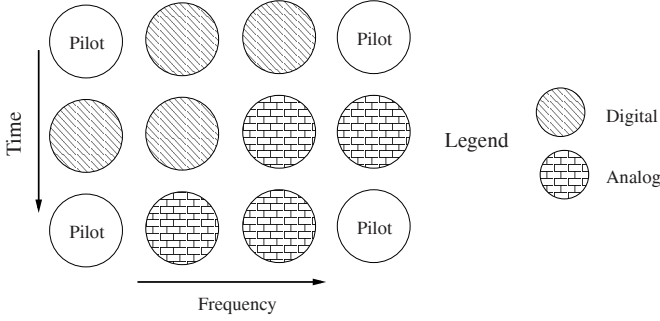


Fig. 2. Tile assignment.

the B quantization bits for each user into a codeword (c_1, \dots, c_n) .

- (6) Send \mathbf{E}_k and (c_1, \dots, c_n) for each user over the uplink channel. This should be done by splitting the resources in the channel, i.e., power and bandwidth, between the analog error signal and the digital code depending on the application. We will show an example of such splitting and the corresponding receiver, using the uplink control channel in the IEEE802.16e standard [26].

At the base station, digital data is decoded using a maximum likelihood (ML) decoder. This will not incur much complexity since the number of quantization bits is small. The analog error signal is reconstructed using a linear MMSE estimator for each analog symbol. Denoting the estimated \mathbf{E}_k by $\hat{\mathbf{E}}_k$ and assuming correct decoding of the digital quantized data, $\hat{\mathbf{V}}_k$ for user k is reconstructed as $\hat{\mathbf{V}}_k = \hat{\mathbf{V}}_k + \hat{\mathbf{E}}_k$.

In order to ensure the correct decoding of the digital quantized data in the hybrid algorithm when we are designing for a SNR_{UL} range of interest, $[\text{SNR}_{\text{min}}, \text{SNR}_{\text{max}}]$, we can design the cardinality of the quantizer codebook based on SNR_{min} and rely on the analog error transmission to provide the additional correction needed when SNR_{UL} is higher.

C. MSE Comparison of Analog and Hybrid Schemes

To see the benefit of using a hybrid scheme compared to an analog scheme with repetition, we can compare the MSE or distortion for the two cases for our multiuser system with rank 1 transmission. For the hybrid scheme we assume that the N_t analog symbols of \mathbf{E}_k are sent over a fraction δ of the $\beta_{fb}N_t$ channel uses. Hence, assuming error free transmission of the digital signal (which is a reasonable assumption if the digital code is designed for SNR_{min}), the MSE per symbol of $\mathbf{v}^{(k)}$ is given only by the MSE of the corresponding analog error symbol after linear MMSE combining. Using the well known formula for a linear MMSE estimator (see for example [39] for a summary),

$$\text{MSE}_H = \frac{\sigma_e^2 / \text{SNR}_{\text{UL}}}{\delta \beta_{fb} \|\mathbf{h}_{\text{UL}}^{(k)}\|^2 \sigma_e^2 + 1 / \text{SNR}_{\text{UL}}} \quad (8)$$

where σ_e^2 is the per symbol variance of the error vector \mathbf{E}_k and MSE_H is the MSE per symbol of $\mathbf{v}^{(k)}$ after hybrid transmission. Here $\mathbf{h}_{\text{UL}}^{(k)}$ denotes the equivalent $N_t \times 1$ uplink channel that each symbol sees and $\delta \beta_{fb}$ is the repetition factor for the analog error symbols in \mathbf{E}_k . We assume that the uplink

channel is block constant during the transmission of a single symbol. Similarly for the analog MSE we have

$$\text{MSE}_A = \frac{\sigma_v^2 / \text{SNR}_{\text{UL}}}{\beta_{fb} \|\mathbf{h}_{\text{UL}}^{(k)}\|^2 \sigma_v^2 + 1 / \text{SNR}_{\text{UL}}} \quad (9)$$

where σ_v^2 is the variance per symbol of $\mathbf{v}^{(k)}$ and MSE_A is the MSE per symbol of $\mathbf{v}^{(k)}$ after analog transmission. Comparing the two expressions we can find that $\text{MSE}_H \leq \text{MSE}_A$ if and only if

$$\frac{1}{\sigma_e^2} - \frac{1}{\sigma_v^2} \geq \|\mathbf{h}_{\text{UL}}^{(k)}\|^2 \text{SNR}_{\text{UL}} \beta_{fb} (1 - \delta) \quad (10)$$

First note that the hybrid scheme could have a performance at least equal to the analog scheme since the analog scheme is a special case of the hybrid scheme when $\delta = 1$. Now fixing a specific channel allocation, δ , we can find the maximum SNR_{UL} , SNR_{max} , for which the above inequality is satisfied. This shows that the hybrid algorithm outperforms the analog using a fixed digital codebook as long as the SNR_{UL} is smaller than this SNR_{max} . As we will show in Section VI, using a small fixed digital codebook, the hybrid algorithm outperforms the analog in a wide range of SNR.

VI. SIMULATIONS

Here we implement the digital, analog, and hybrid feedback algorithms in a multiuser system with 4 users and a transmitter with $N_t = 4$ antennas and in two scenarios: First, in a simple case where the uplink channel is an unfaded SIMO Gaussian channel (or equivalently an AWGN channel with $N_t \text{SNR}_{\text{UL}}$) and each of the 4 users have 1 antenna. Then in the realistic case where the uplink channel is a Rayleigh faded SIMO Gaussian channel generated according to the power delay profile of the ITU Pedestrian B channel [33] and each user has 2 receive antennas and transmits with 1 fixed antenna in the uplink (as is the case in most wireless devices). In this case we assume a mobile speed of 3 km/hr as is typically used in cellular system simulations for pedestrian speed and simulate the channel using a modified Jakes model for Rayleigh fading as in [34].

A. Simulation Setup

We use the uplink control channel in the IEEE 802.16e standard [26] for our implementation. This channel consists of basic units, called tiles, each consisting of 12 uses of the uplink channel, 4 for pilots and 8 for data as shown in Fig. 2¹.

For the case of multiuser MIMO implementation, rank 1 transmission is used and hence each user's feedback consists of 4 symbols of $\mathbf{v}^{(k)}$. Hence each tile use of the control channel

¹Note that we considered a channel with 10 MHz bandwidth at the carrier frequency of 2.5 GHz and used an FFT size of 1024 (number of subcarriers) in our implementation. This means that each channel use in the uplink is approximately 100 μs and 11 kHz in the time and frequency dimensions respectively. For the case of the ITU Pedestrian B channel with 3 km/hr speed, one can calculate the time and frequency coherence and show that in this case each tile goes through approximately a constant fade. However, since $N_t = 4$, the feedback symbols see N_t independent fades in the uplink. Hence the uplink is approximately a Rayleigh block-fading $N_t \times 1$ channel. This also means that the feedback duration is $T_f = 300 \mu\text{s}$ and hence much smaller than the coherence time, T_c , that is in the order of 10's of $m\text{s}$.

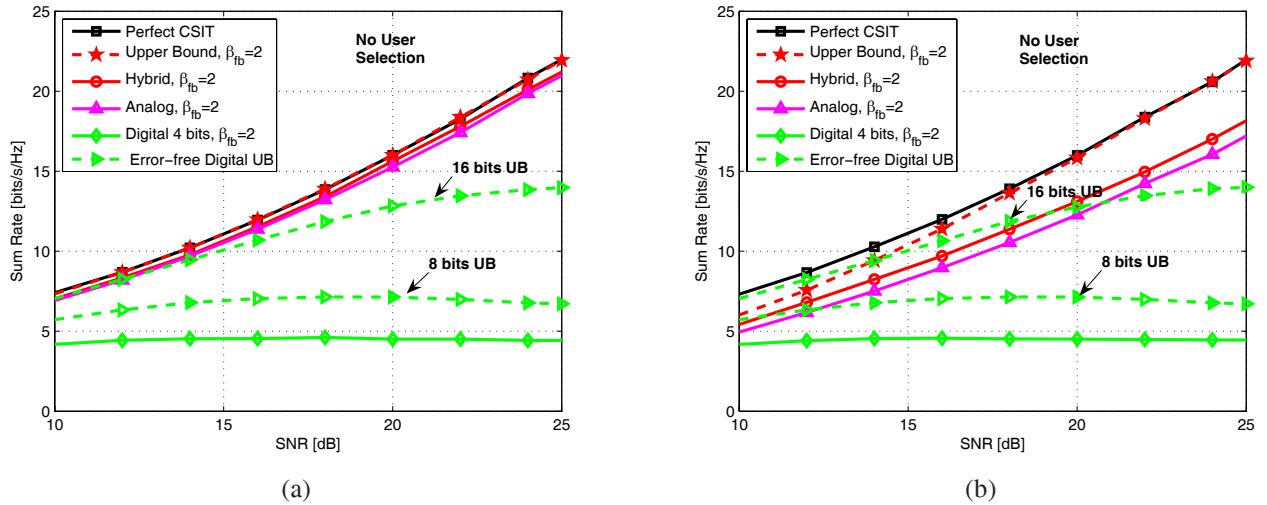


Fig. 3. Sum rates for the 4 user system with 1×4 downlink channels and AWGN uplink channels (of $N_t \text{SNR}_{UL}$) without user selection and with (a) $\Delta \text{SNR} = 6$ dB (b) $\Delta \text{SNR} = 15$ dB.

corresponds to a $\beta_{fb} = 2$. In the hybrid scheme, the digital data is constructed using the 4 bit codebook quantizer in [40] which has similar performance to the codebooks adapted in the Long Term Evolution (LTE) standard [41]. To encode the 4 bits, we use the (8,4,4) extended Hamming code. These 8 coded bits are then placed on 4 (complex) channel uses within a tile and the other 4 channel uses are used for analog transmission of the error signal as shown in Fig. 2, i.e., here $\delta = 0.5$.

We satisfy the uplink power constraint of P_{UL} per channel use by scaling each tile with a factor α which depends on the analog error power in that tile. However since the analog error variance (average power) is much smaller than the constant digital power of 1 per symbol (QPSK constellation), we first boost the analog error signal by a *known* factor γ which we optimize over. Hence, the power equation for a tile becomes $P_{UL} = (\alpha^2/8)(P_{\text{digital}} + \gamma^2 \|E\|_F^2)$, where $P_{\text{digital}} = 4$ (4 QPSK symbols) and from which we can obtain α for any tile. At the receiver we estimate α (required to retrieve the magnitude of the analog error) by finding the ratio of pilot to digital average power since pilots all have power 1.

The encoding in the pure 4 bits digital scheme is the same as the digital part of the hybrid scheme discussed above. For both the pure analog and pure digital schemes, each symbol of the feedback is just repeated twice within a tile and the appropriate power scaling is used. Since here only the direction matters, there is no need to estimate this factor at the base station.

We also run simulations according to the procedures described in Sections III and IV to find upper-bounds on the performance of the system and also error-free and outage-aware upper-bounds on the performance of the digital scheme for different codebook cardinalities.

B. Simulation Results

Fig. 3 and 4 compare the overall throughputs of the analog and hybrid schemes vs. downlink SNR in the two simulation scenarios for $\Delta \text{SNR} = 6$ dB and 15 dB, with and without user selection and for $\beta_{fb} = 2$. In these figures we also show the

random VQ upper-bound on the performance of the system, assuming error free transmission at *capacity* as described in Section III. We also show the performance of the 4 bit digital scheme and error-free upper-bounds on the performance of fixed digital approaches with 8 and 16 bits. Note that the error-free upper-bounds by definition are independent of ΔSNR in contrast to outage-aware upper-bounds.

Fig. 3 compares the different algorithms for the first scenario without user selection. At $\Delta \text{SNR} = 6$ dB, both analog and hybrid transmissions perform very close to perfect CSIT. Note that hybrid transmission performs better than analog and this improvement becomes more apparent at larger ΔSNR . Also the performance of the hybrid algorithm is very close to the system upper-bound for up to about 15 dB even for $\Delta \text{SNR} = 15$ dB and better than analog by about 1 dB at this ΔSNR . Note that the error-free upper-bounds on digital shown here are very loose at SNR values where user uplink is in outage.

Fig. 4 similarly shows the throughputs for the second simulation scenario with and without user selection. We again observe that both analog and hybrid perform very close to perfect CSIT and hybrid performs better than analog as ΔSNR grows. For example at $\Delta \text{SNR} = 15$ dB hybrid is 1 dB better than analog in most regimes. The improvement of hybrid over analog repetition results from the fact that the analog error has a much lower variance (about 5 dB lower) than the signal itself. Hence sending the error as opposed to repeating the signal over the same channel results in a lower MSE in signal reconstruction (cf. Section V-C). Again here error-free upper-bounds are shown on the performance of the digital. We can see that the digital approach with any fixed number of bits and no user selection saturates in both simulation scenarios as expected [8], and with user selection, even though it does not saturate, it still has a substantial loss as compared to perfect CSIT.

To compare the separation based and non-separation based schemes, in Fig. 5, we have shown outage-aware upper-bounds on the performance of the digital which are tighter

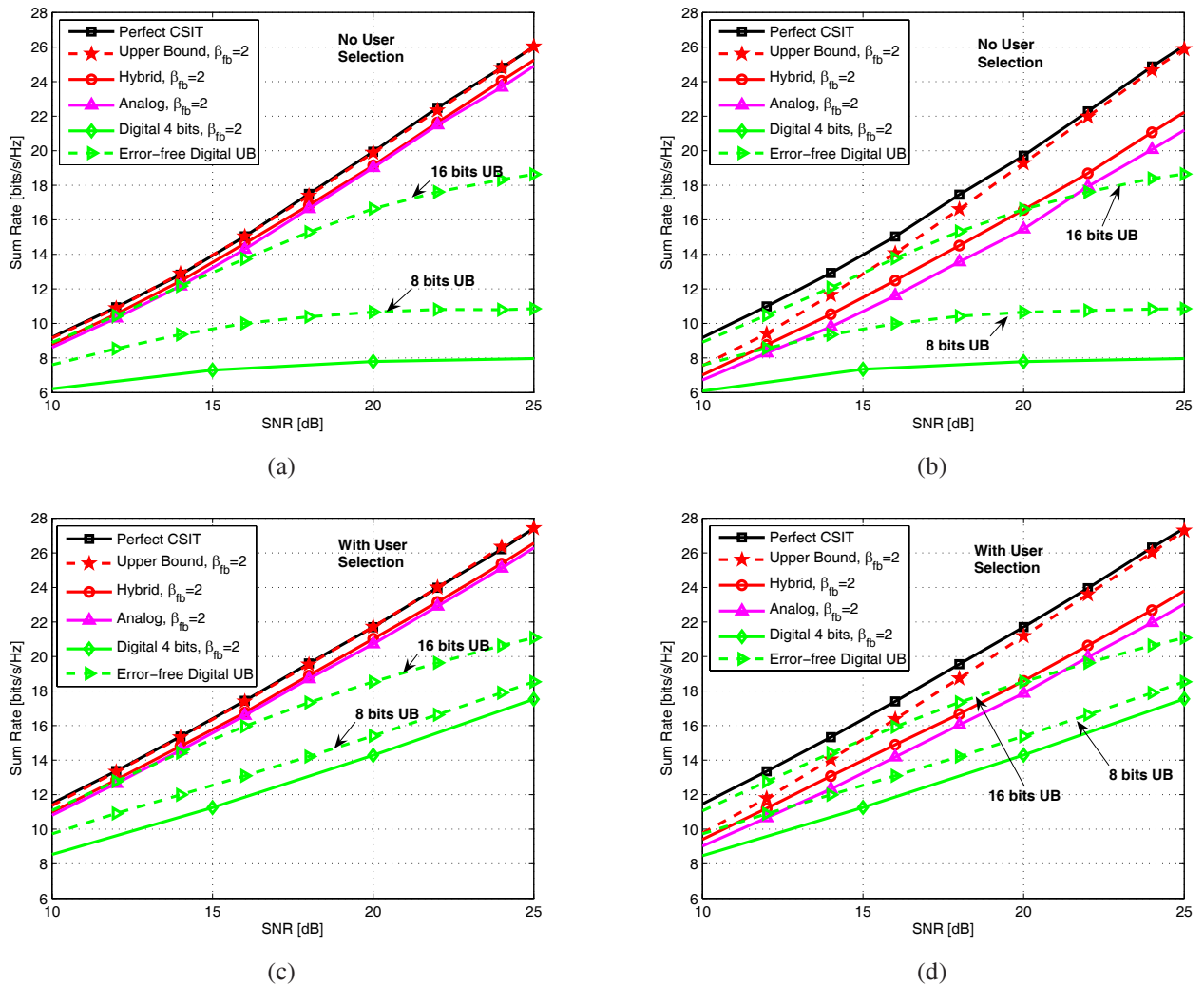


Fig. 4. Sum rates for the 4 user system with 2×4 downlink channels and faded SIMO uplink channels and with (a) no user selection and $\Delta\text{SNR} = 6$ dB (b) no user selection and $\Delta\text{SNR} = 15$ dB (c) user selection and $\Delta\text{SNR} = 6$ dB (d) user selection and $\Delta\text{SNR} = 15$ dB.

than the error free upper-bounds at lower SNRs. Also shown is the outage-aware envelope of the digital performance for codebooks of size 5 bits to 25 bits over the entire SNR range again assuming random VQ error free transmission while not in outage (even though short block lengths have to be used). This envelope shows the best possible performance of a digital scheme with variable codebook size, where the size of the codebook is optimized at all SNR points. The outage-aware upper-bounds clearly show the threshold effect of the digital approach. We can also see that even using a variable size digital approach, for a wide range up to about 19 dB, the hybrid algorithm outperforms digital. We can simply modify our hybrid algorithm by picking a larger digital codebook component to further improve its performance at higher SNR regimes. Note that in contrast to the digital scheme, the performance of the hybrid scheme is not sensitive to the cardinality of the codebook used. For example, using a single 4 bit codebook, the hybrid has better performance than both digital and analog over a wide range up to 19 dB.

In terms of practical implementation, note that for the hybrid algorithm, a single small codebook of 4 bits is used whereas

for the digital envelope the codebook size changes from 5 bits up to 25 bits depending on the SNR. This requires the design of multiple codebooks of large cardinality which in turn have a much greater decoding complexity as compared to a simple analog or hybrid scheme. Moreover, as discussed before, the exact SNR is unknown and users may not have a good estimate of it. Also, in practice a limited number of codebooks (with different sizes) would be used and thus a single codebook would need to be used for a range of SNRs, limiting the granularity of the number of operational SNR points. Both the SNR estimation error and limited SNR granularity, will degrade the performance of such a digital approach. We conjecture that in practice, the loss from these factors will be more pronounced than that associated with even using a simple analog scheme. Moreover, by using the hybrid scheme we can further reduce the gap in performance from that of perfect CSIT.

Note that the setup we consider is one with small to moderate bandwidth expansion ratios where the number of analog symbols sent is on the order of the number of channel symbols. This regime is motivated by typical setups considered

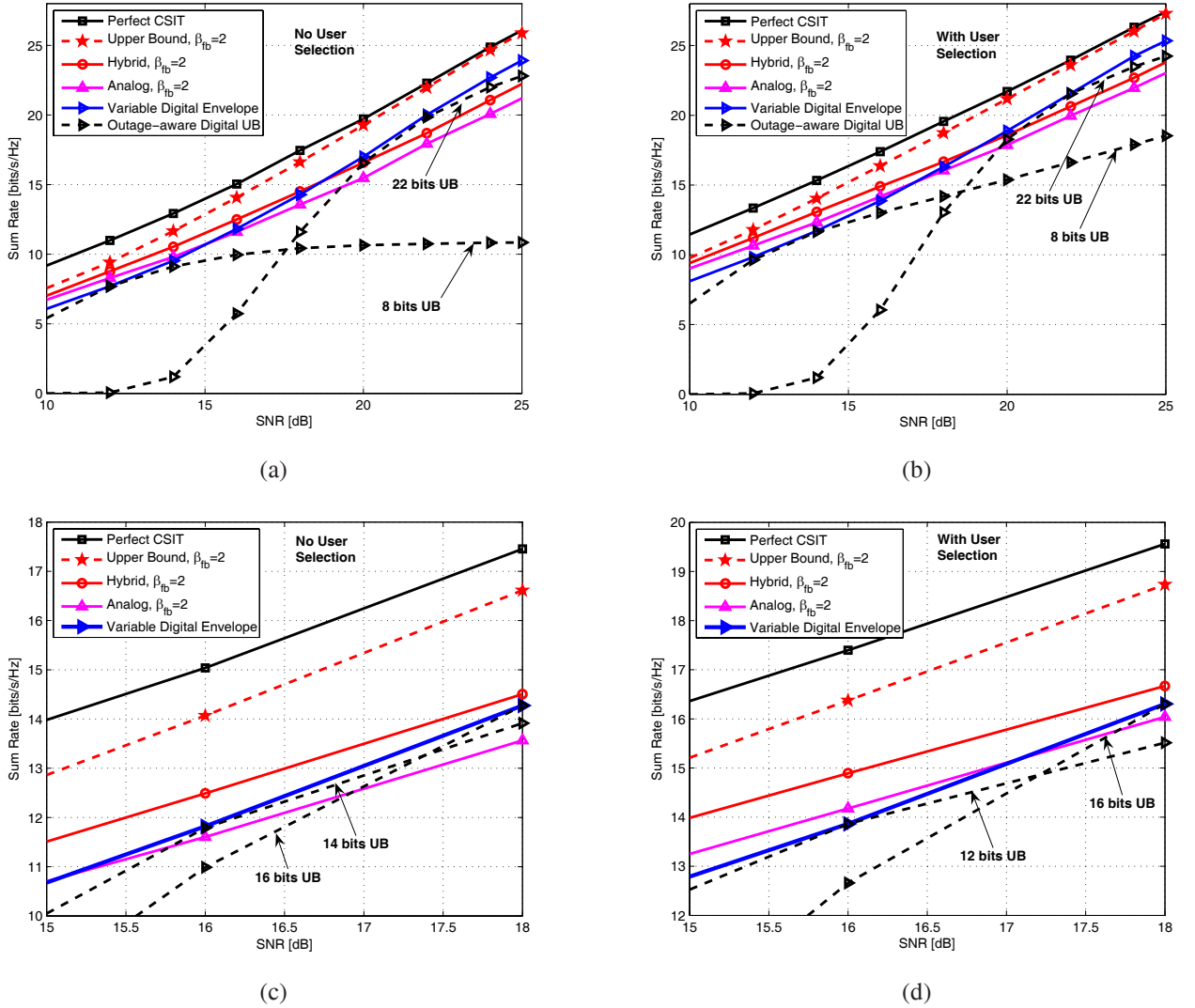


Fig. 5. Sum rates for the 4 user system with 2×4 downlink channels and faded SIMO uplink channels and with $\Delta\text{SNR} = 15$ dB and (a) no user selection, (c) no user selection zoomed in, (b) user selection, and (d) user selection zoomed in.

in wireless systems such as WiMAX [26] to efficiently allocate uplink resources to the users served as also considered in [11], [13], [14]. In a regime with large β_{fb} however, we expect the performance of a digital scheme to surpass that of an analog scheme since analog repetition becomes inefficient in such a regime.

VII. CONCLUSION

We examined the relative merits of separation-based and non-separation based transmission schemes in the context of multiuser MIMO channel feedback and showed that non-separation based schemes are preferable for this application when small to moderate bandwidth expansion ratios are used. Among non-separation schemes, we developed a hybrid digital-analog feedback scheme that achieves higher throughputs compared to pure analog or digital schemes and also has a much smaller computational complexity compared to a purely digital approach.

APPENDIX

The objective is to find $\Phi_{\text{opt}}^{(k)} = \arg \min_{\Phi \in \mathcal{U}} \|\bar{\mathbf{V}}_k - \mathbf{V}_k \Phi\|_F^2$. We can write

$$\begin{aligned} \|\bar{\mathbf{V}}_k - \mathbf{V}_k \Phi\|_F^2 &= \text{trace} \left((\bar{\mathbf{V}}_k - \mathbf{V}_k \Phi)^\dagger (\bar{\mathbf{V}}_k - \mathbf{V}_k \Phi) \right) \\ &= \text{trace} \left(\bar{\mathbf{V}}_k^\dagger \bar{\mathbf{V}}_k - \bar{\mathbf{V}}_k^\dagger \mathbf{V}_k \Phi - \Phi^\dagger \mathbf{V}_k^\dagger \bar{\mathbf{V}}_k \right. \\ &\quad \left. + \Phi^\dagger \mathbf{V}_k^\dagger \mathbf{V}_k \Phi \right) \\ &= \text{trace} \left(2\mathbf{I} - \bar{\mathbf{V}}_k^\dagger \mathbf{V}_k \Phi - \Phi^\dagger \mathbf{V}_k^\dagger \bar{\mathbf{V}}_k \right) \quad (11) \end{aligned}$$

Writing the singular value decomposition of the correlation matrix, $\mathbf{C} = \bar{\mathbf{V}}_k^\dagger \bar{\mathbf{V}}_k = \mathbf{U}_{\text{corr}} \Sigma \mathbf{V}_{\text{corr}}^\dagger$, and using (11), the

optimum unitary transformation $\Phi_{\text{opt}}^{(k)}$ is given by

$$\begin{aligned}\Phi_{\text{opt}}^{(k)} &= \arg \max_{\Phi \in \mathcal{U}} \text{trace} \left(\bar{\mathbf{V}}_k^\dagger \mathbf{V}_k \Phi + \Phi^\dagger \mathbf{V}_k^\dagger \bar{\mathbf{V}}_k \right) \\ &= \arg \max_{\Phi \in \mathcal{U}} \text{trace} \left(\text{Re}(\bar{\mathbf{V}}_k^\dagger \mathbf{V}_k \Phi) \right) \\ &= \arg \max_{\Phi \in \mathcal{U}} \text{trace} \left(\text{Re}(\mathbf{U}_{\text{corr}} \Sigma \mathbf{V}_{\text{corr}}^\dagger \Phi) \right) \\ &= \arg \max_{\Phi \in \mathcal{U}} \text{trace} \left(\text{Re}(\Sigma \mathbf{V}_{\text{corr}}^\dagger \Phi \mathbf{U}_{\text{corr}}) \right)\end{aligned}$$

Now since $\mathbf{V}_{\text{corr}}^\dagger \Phi \mathbf{U}_{\text{corr}}$ is unitary and Σ is a diagonal matrix with non-negative real diagonal entries, the real part of the trace is maximized if $\Sigma \mathbf{V}_{\text{corr}}^\dagger \Phi \mathbf{U}_{\text{corr}}$ is diagonal with $\mathbf{V}_{\text{corr}}^\dagger \Phi \mathbf{U}_{\text{corr}} = \mathbf{I}$ and hence $\Phi_{\text{opt}}^{(k)} = \mathbf{V}_{\text{corr}} \mathbf{U}_{\text{corr}}^\dagger$.

ACKNOWLEDGMENT

The authors would like to thank Dr. Yi Jiang for valuable discussions.

REFERENCES

- [1] J. Zhang, J. G. Andrews, and R. W. Heath, "Single-user MIMO vs. multiuser MIMO in the broadcast channel with CSIT constraints," in *Allerton Conf. Commun., Contr., Comput.*, 2008.
- [2] A. Lapidoth, S. Shamai(Shitz), and M. A. Wigger, "On the capacity of fading MIMO broadcast channels with imperfect transmitter side-information," *IEEE Trans. Inf. Theory*, May 2006.
- [3] G. Caire, N. Jindal, and S. Shamai, "On the required accuracy of transmitter channel state information in multiple-antenna broadcast channels," in *Asilomar Conf. Signals, Syst. Comput.*, 2007.
- [4] D. J. Love and R. W. Heath, "Limited feedback unitary precoding for spatial multiplexing systems," *IEEE Trans. Inf. Theory*, vol. 51, no. 8, pp. 2967-2976, Aug. 2005.
- [5] D. Love, R. W. Heath, and T. Strohmer, "Grassmannian beamforming for multiple-input multiple-output wireless systems," *IEEE Trans. Inf. Theory*, vol. 49, no. 10, pp. 2735-2747, Oct. 2003.
- [6] A. D. Dabagh and D. J. Love, "Feedback rate-capacity loss tradeoff for limited feedback MIMO systems," *IEEE Trans. Inf. Theory*, vol. 52, no. 5, pp. 2190-2202, May 2006.
- [7] P. Ding, D. Love, and M. Zoltowski, "Multiple antenna broadcast channels with shape feedback and limited feedback," *IEEE Trans. Signal Process.*, vol. 55, no. 7, pp. 3417-3428, July 2007.
- [8] N. Jindal, "MIMO broadcast channels with finite rate feedback," *IEEE Trans. Inf. Theory*, vol. 52, no. 11, pp. 5045-5059, Nov. 2006.
- [9] G. Caire, N. Jindal, M. Kobayashi, and N. Ravindran, "Multiuser MIMO downlink made practical: achievable rates with simple channel state estimation and feedback schemes," *IEEE Trans. Inf. Theory*, Nov. 2007, submitted for publication. [Online]. Available: <http://arxiv.org/abs/0711.2642>.
- [10] R. G. Gallager, *Information Theory and Reliable Communication*. New York: Wiley, 1968.
- [11] T. A. Thomas, K. L. Baum, and P. Sartori, "Promising feedback methods for transmit beamforming in broadband mobile OFDM," in *IEEE WCNC*, 2006.
- [12] T. L. Marzetta and B. M. Hochwald, "Fast transfer of channel state information in wireless systems," *IEEE Trans. Signal Process.*, vol. 54, no. 4, pp. 1268-1278, Apr. 2006.
- [13] D. Samardzija and N. Mandayam, "Unquantized and uncoded channel state information feedback in multiple-antenna multiuser systems," *IEEE Trans. Commun.*, vol. 54, no. 7, pp. 1335-1345, July 2006.
- [14] E. Chiu, P. Ho, and J. H. Kim, "Transmit beamforming with analog channel state information feedback," *IEEE Trans. Wireless Commun.*, vol. 7, no. 3, pp. 878-887, Mar. 2008.
- [15] M. Gastpar, B. Rimoldi, and M. Vetterli, "To code, or not to code: lossy source-channel communication revisited," *IEEE Trans. Inf. Theory*, vol. 49, no. 5, pp. 1147-1158, May 2003.
- [16] T. J. Goblick, "Theoretical limitations on the transmission of data from analog sources," *IEEE Trans. Inf. Theory*, vol. IT-11, pp. 558-567, Oct. 1965.
- [17] U. Mittal and N. Phamdo, "Hybrid digital-analog (HDA) joint source-channel codes for broadcasting and robust communications," *IEEE Trans. Inf. Theory*, vol. 48, no. 5, pp. 1082-1102, May 2002.
- [18] N. Phamdo, N. Farvardin, and T. Moriya, "A unified approach to tree-structured and multistage vector quantization for noisy channels," *IEEE Trans. Inf. Theory*, vol. 39, no. 2, pp. 835-850, May 1993.
- [19] M. Wang and T. R. Fischer, "Trellis-coded quantization designed for noisy channels," *IEEE Trans. Inf. Theory*, vol. 40, no. 6, p. 17921802, Nov. 1994.
- [20] M. Skoglund, N. Phamdo, and F. Alajaji, "Hybrid digital-analog source-channel coding for bandwidth compression/expansion," *IEEE Trans. Inf. Theory*, vol. 52, no. 8, pp. 3757-3763, Aug. 2006.
- [21] G. Jongren and M. Skoglund, "Quantized feedback information in orthogonal space-time block coding," *IEEE Trans. Inf. Theory*, vol. 50, no. 10, pp. 2473-2482, Oct. 2004.
- [22] S. Ekbatani and H. Jafarkhani, "Combining beamforming and space-time coding using noisy quantized feedback," *IEEE Trans. Commun.*, vol. 57, no. 5, pp. 1280-1286, May 2009.
- [23] S. Yao and M. Skoglund, "Hybrid digital-analog relaying for cooperative transmission over slow fading channels," *IEEE Trans. Inf. Theory*, vol. 55, no. 3, pp. 944-951, Mar. 2009.
- [24] V. Prabhakaran and K. Ramchandran, "Hybrid digital-analog codes for source-channel broadcast of Gaussian sources over Gaussian channels," *IEEE Trans. Inf. Theory*, 2009.
- [25] G. Caire and K. R. Narayanan, "On the SNR exponent of hybrid digital analog space time codes," in *Proc. 43rd Annu. Allerton Conf. Commun., Control Comput.*, Monticello, IL, Oct. 2005.
- [26] IEEE P802.16Rev2, "Standard for local and metropolitan area networks part 16: air interface for broadband wireless access systems," 2008.
- [27] F. Boccardi, H. Huang, and M. Trivellato, "Multiuser eigenmode transmission for MIMO broadcast channels with limited feedback," in *SPAWC Workshop*, 2007.
- [28] C. B. Peel, B. M. Hochwald, and A. L. Swindlehurst, "A vector-perturbation technique for near-capacity multiantenna multiuser communication-part I: channel inversion and regularization," *IEEE Trans. Commun.*, vol. 53, no. 1, pp. 195-202, Jan. 2005.
- [29] H. Weingarten, Y. Steinberg, and S. Shamai, "The capacity region of the Gaussian multiple-input multiple-output broadcast channel," *IEEE Trans. Inf. Theory*, vol. 52, no. 9, pp. 3936-3964, Sep. 2006.
- [30] S. Vishwanath, N. Jindal, and A. Goldsmith, "Duality, achievable rates, and sum-rate capacity of Gaussian MIMO broadcast channels," *IEEE Trans. Inf. Theory*, vol. 49, no. 10, pp. 2658-2668, Oct. 2003.
- [31] G. Caire and S. Shamai, "On the achievable throughput of a multi-antenna Gaussian broadcast channel," *IEEE Trans. Inf. Theory*, vol. 49, no. 7, pp. 1691-1706, July 2003.
- [32] T. Yoo and A. Goldsmith, "On the optimality of multiantenna broadcast scheduling using zero-forcing beamforming," *IEEE J. Sel. Areas Commun.*, vol. 24, no. 3, pp. 528-541, Mar. 2006.
- [33] ITU-R, "Guidelines for evaluation of radio transmission technologies for IMT-2000," 1997. [Online]. Available: <http://www.itu.int/rec/R-REC-M.1225-0-199702-I/en>. [Accessed Feb. 26, 2009].
- [34] Y. R. Zheng and C. Xiao, "Improved models for the generation of multiple uncorrelated Rayleigh fading waveforms," *IEEE Commun. Lett.*, vol. 6, no. 6, pp. 256-258, June 2002.
- [35] ITU-R, "Guidelines for evaluation of radio interface technologies for IMT-advanced," 2008. [Online]. Available: www.itu.int/publ/R-REP-M.2135-2008/en. [Accessed Feb. 26, 2009].
- [36] N. Jindal, "Antenna combining for the MIMO downlink channel," *IEEE Trans. Wireless Commun.*, vol. 7, no. 10, pp. 3834-3844, Oct. 2008.
- [37] C. K. Au-Yeung and D. J. Love, "On the performance of random vector quantization limited feedback beamforming in a MISO system," *IEEE Trans. Wireless Commun.*, vol. 6, no. 2, pp. 458-462, Feb. 2007.
- [38] M. Skoglund, N. Phamdo, and F. Alajaji, "Design and performance of VQ-based hybrid digital-analog joint source-channel codes," *IEEE Trans. Inf. Theory*, vol. 48, no. 3, pp. 708-720, Mar. 2002.
- [39] D. Tse and P. Viswanath, *Fundamentals of Wireless Communication*. New York: Cambridge University Press, 2005.
- [40] R. Porat, "Proposal for a 4-antenna codebook," IEEE 802.16 Broadband Wireless Access Working Group, Sep. 2008. [Online]. Available: <http://www.ieee802.org/16/tgm/contrib/16/tgm/contrib/C80216m-08\916.pdf>. [Accessed Feb. 26, 2009].
- [41] "3GPP TS 36.211 V8.5.0 technical specification," 2008. [Online]. Available: <http://www.3gpp.org/ftp/Specs/archive/36\series/36.211/36211-850.zip>. [Accessed Feb. 26, 2009].



Maryam M. Shanechi received the B.A.Sc. degree (with honors) in Engineering Science (Electrical Option) from the University of Toronto in 2004 and the S.M. degree in Electrical Engineering and Computer Science from the Massachusetts Institute of Technology (MIT) in 2006, where she is currently pursuing the Ph.D. degree. Her research interests are in the areas of communications, information theory, statistical signal processing, and computational neuroscience. She has received various awards for academic achievement including the Professional

Engineers of Ontario (PEO) gold medal and the Wilson Medal. She holds a Natural Sciences and Engineering Research Council of Canada (NSERC) doctoral fellowship. She has held internships at Altera Corp., Vanu, Inc., NextWave Wireless, Inc., and HP Labs.



Ron Porat received the BS Summa Cum Laude and MS all in Electrical Engineering from the Technion, Israel Institute of Technology in 1990 and 1994 respectively. He is currently a Principal DSP Engineer at Broadcom Corporation San Diego, CA. Prior to that he held positions with InterDigital Communications, Mitsubishi Electric Research Labs, Nextwave, Entropic Communications and Qualcomm working on diverse communication systems and standards such as Globalstar, Gigabit Ethernet, 802.11, MoCA, WiMAX and LTE. His research interests are in the

areas of communication systems and array signal processing. He is a member of the IEEE. He can be reached at rporat@broadcom.com



Uri Erez was born in Tel Aviv, Israel, on October 27, 1971. He received the B.Sc. degree in mathematics and physics and the M.Sc. and Ph.D. degrees in electrical engineering from Tel Aviv University in 1996, 1999, and 2003, respectively. During 2003-2004, he was a Postdoctoral Associate at the Signals, Information and Algorithms Laboratory at the Massachusetts Institute of Technology (MIT), Cambridge. Since 2005, he has been with the Department of Electrical Engineering-Systems at Tel Aviv University. His research interests are in

the general areas of information theory and digital communication. He is currently an Associate Editor for IEEE TRANSACTIONS ON INFORMATION THEORY.